# Passive seismic reservoir monitoring techniques applied to heavy oil production

Jeffrey F. Tan, Henry C. Bland and Robert R. Stewart

## ABSTRACT

The CREWES project at the University of Calgary is conducting research with Imperial Oil Limited concerning passive seismic monitoring of heavy oil production wells at Cold Lake, Alberta. Research is involved with developing algorithms and techniques to improve the current classification application being used. Passive seismic event classification algorithms that involve frequency filtering, statistical analysis, and event length detection, are developed here and combined into a Graphical User Interface application intended for use in reservoir monitoring. Initial testing on the developed application, which was in progress at the time this paper was written, has produced encouraging results. More testing remains to be done.

## INTRODUCTION

Imperial Oil Ltd. is currently performing passive seismic monitoring at Cold Lake, Alberta to detect microseismic earthquakes that could be induced by a Cyclic Steam Stimulation (CSS) process (Campbell, 2005). The CSS process is required to extract the viscous bitumen, which has an American Petroleum Institute (API) index of approximately 8° to 9º. Passive seismic monitoring of these microseisms can proactively detect anomalies during production. This can minimize potential economic and environmental costs that may result from undesirable production events such as casing failures or cement cracks. These events can be caused by the high temperatures and pressures involved in the CSS process which are approximately 320 °C and 11 MPa, respectively (Campbell, 2005). If undetected, these production issues could potentially cause environmental damage such as aquifer contamination. The CREWES Project at the University of Calgary is involved in this passive seismic research with Imperial Oil Ltd. A map depicting the location of the Cold Lake operations is shown in Figure 1 (Imperial Oil Ltd., 2006).

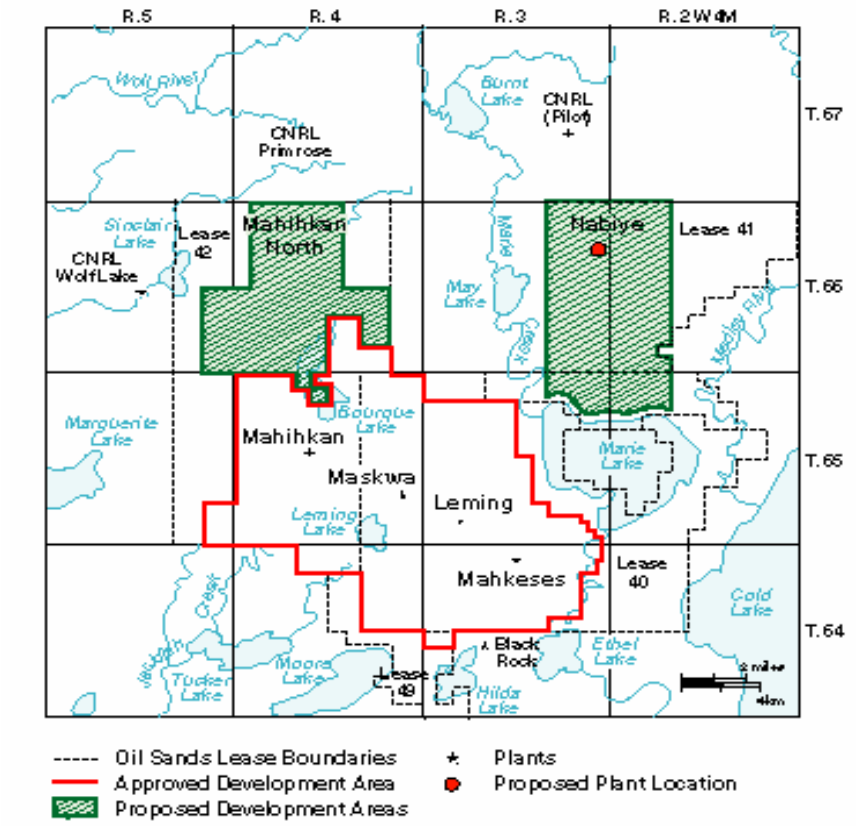


FIG. 1. Location of Imperial Oil's Cold Lake operations.

Imperial Oil Ltd. has implemented passive seismic monitoring on approximately 75 production pads, each of which contain about 18 to 24 producing wells. Each pad has one centrally located monitoring well that records ground vibrations (including microseisms). The monitoring well is instrumented by a down-hole array of 3-component geophone sondes connected to seismic recorders at the surface. Recording equipment is comprised of a mixture of systems from Terrascience Systems Ltd. and ESG Inc. The recording equipment, connected to a down-hole geophone array, listens for discrete seismic events and stores them to disk for later review. These digital event files typically contain a 1.5 second time sample of microseismic activity recorded by the entire down-hole array.

Vendor-supplied event-classification software analyzes each one of these files and assigns them a classification. If a file is classified as "good", this is intended to indicate that the event detected warrants further investigation; conversely, if the file is classified as "noise", it is supposedly an event that is not of interest (approximately 99% of all detected events are noise). Examples of "good" events worth further investigation include cement cracks around the casing in the wells, and casing failures. Examples of noise events include noise created by pump rods and vehicles passing (Campbell, 2005). Generally, noise events are not important and are usually discarded.

The current event-file classification software has been known to misclassify a large portion of the received files. This has resulted in "good" events and noise events being incorrectly identified. These numerous misclassifications can become very costly, as significant time is required to manually investigate the files one by one.

The purpose of this research is to develop and combine microseismic event classification algorithms that classify the detected events with a high accuracy. We explore algorithms that include frequency filtering, event-length detection, and statistical analysis. An interactive Graphical User Interface (GUI) application containing these algorithms is developed and tested. This GUI application is undergoing testing and optimization, but initial tests performed have yielded reasonably strong results.

## METHODOLOGY

Algorithms developed in this research are combined to classify microseismic event files into two categories: useful events worth further investigation ("good" events), and noise events. This classification is based on the aggregate results of these algorithms, which include the following:

- Filtering techniques (low-pass filtering, high-pass filtering, and band-pass filtering).
- Statistical analysis of the signal.
- Event length detection using frequency and time domain analysis.

Each analysis algorithm is applied to each of the traces of an event file. These traces correspond to all three triaxial geophone outputs for all of the levels within a single monitoring well. Results from the algorithms are coded as "1" if the algorithm deems the trace to contain a "good" event, and "0" otherwise. The algorithm results are summed on a per-trace basis providing a per-trace score. Those traces which have a score exceeding a threshold are flagged as "good" while the remaining traces are flagged as "noise". The overall file classification is determined by identifying the total number of "good" traces. Deciding upon the exact threshold classification values pertaining to the various algorithms is empirically determined and is adjustable to various datasets.

## EXAMPLE EVENTS

Before discussing the details of the algorithms used, two sample traces are shown in Figures 2 and 3. A trace obtained from a "good" event, with the P- and S-wave arrivals indicated, is shown in Figure 2. A trace obtained from a noise event is shown in Figure 3. These two example traces will be used when demonstrating and discussing most of the algorithms. These two traces do not characterize all of the possible detected events, but are a fairly reasonable representation of the characteristics pertaining to a fair number of "good" and noise events. The traces shown have their amplitudes normalized with any DC offset removed.

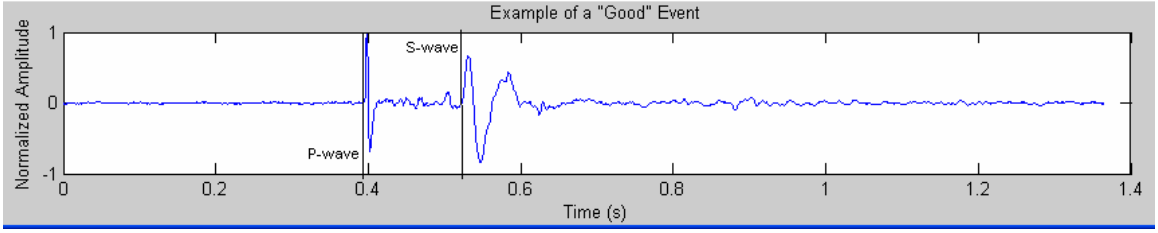


FIG. 2. Example trace obtained from a “good” event.

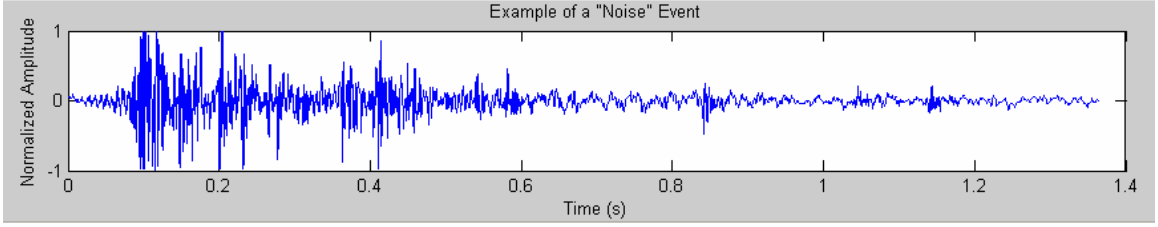


FIG. 3. Example trace obtained from a noise event.

## ALGORITHMS

### Frequency filtering

When examining the passive seismic event files, we found that many noise event channels generally contained a greater quantity of high frequency content than most "good" channels. The first set of algorithms concerns filtering the received signals with low-pass, high-pass, and band-pass filters, followed by an analysis of the filtered signal. Based on the peak value of the output signal, the channel examined is classified as either a noise channel, or a "good" channel.

#### *Filter frequency responses*

To begin, some background on filter design and terminology is provided. One of the most important filter design parameters is the *passband*. The passband is the frequency range where, ideally, the frequency components of the signal experience zero attenuation. The *stopband* is the frequency range where, ideally, the signal is completely attenuated and the frequency components of the signal are eliminated. The *order* of the filter is the order of the characteristic differential equation that describes its impulse response in the time domain. When performing frequency analysis, it is usually desired to analyze these characteristics in the frequency domain. A filter’s impulse response in the time domain corresponds to its transfer function in the frequency domain. In the frequency domain, the order of a filter is the highest power of the Laplace operator "*s*" that can be seen in the denominator of its transfer function. In real applications, as the desired accuracy of a filter increases, its required order increases as well. As the order of a filter increases, its realization increases in complexity. More components are required to construct high order filters. Thus, there is a tradeoff between filter accuracy and complexity.

In practical applications, there are four main types of filter responses that rely on approximations (Maundy, 2005). The Butterworth response contains a maximally flat

attenuation characteristic in the passband (as frequency increases) and a monotonically increasing attenuation characteristic in the stopband. This type of response is known as a maximally flat approximation. The Chebyshev response contains an *equiripple* attenuation characteristic in the passband and a monotonically increasing attenuation characteristic in the stopband. This equiripple characteristic that is present in the Chebyshev (but not the Butterworth) approximation, results in a small oscillation of the frequency response. The Inverse-Chebyshev response contains a maximally flat attenuation characteristic in the passband and an equiripple attenuation characteristic in the stopband. Finally, the Elliptic (also known as the Cauer) response provides an equiripple attenuation characteristic in the passband and the stopband. These filter response characteristics and approximations are needed should it be decided to implement and realize these filters in a hardware capacity at the front end of the passive seismic monitoring system in the future. Currently, models of these filter responses are implemented in MATLAB.

Table 1 summarizes the various responses of the filters. Figure 4 (Maundy, 2005) depicts the attenuation characteristics of these four filter types. In Figure 4, $\omega_p$ and $\omega_s$ represent the passband and stopband limits, respectively. The quantity $\alpha(\omega)$ signifies the attenuation of the filter (in dB) as a function of the radial frequency. The symbols $\alpha_{min}$ and $\alpha_{max}$ are the desired minimum and maximum allowable attenuations in the stopband and passband, respectively.

Table 1. Approximation characteristics of 4 main filter responses.

| Filter Type | Passband Response | Stopband Response |
|---|---|---|
| Butterworth | Maximally Flat | Monotonically Increasing |
| Chebyshev | Equiripple | Monotonically Increasing |
| Inverse Chebyshev | Maximally Flat | Equiripple |
| Elliptic (Cauer) | Equiripple | Equiripple |

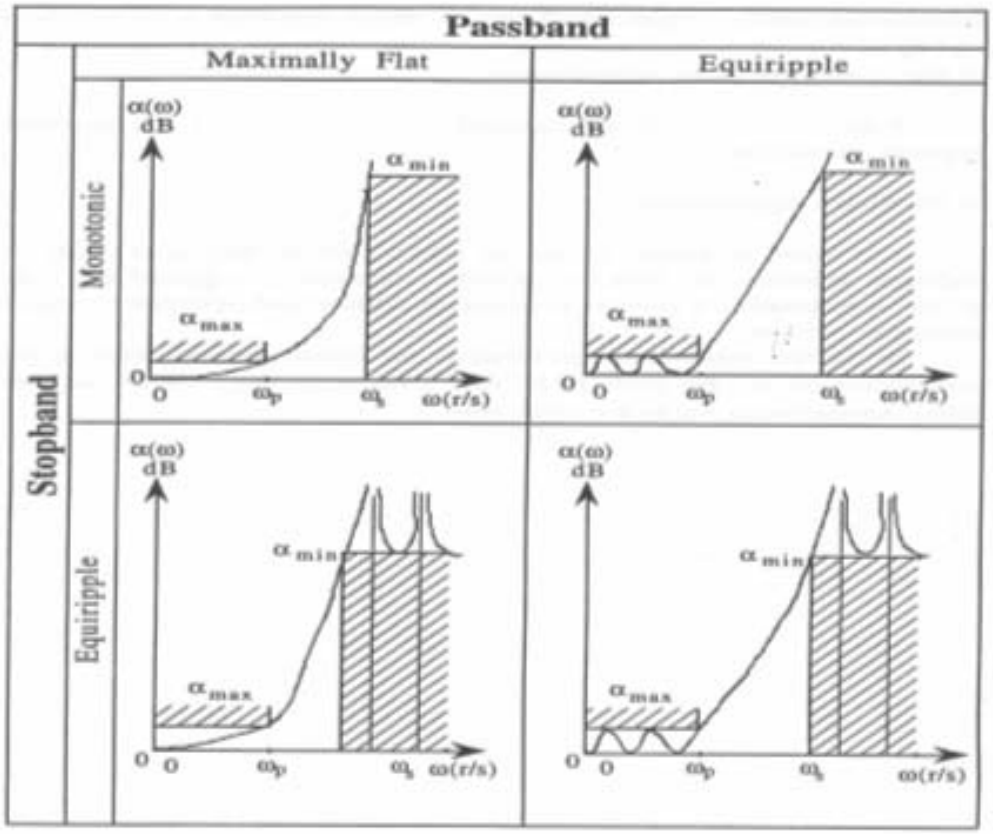


FIG. 4. Attenuation characteristics of 4 main filter responses: Butterworth (top-left), Chebyshev (top-right), Inverse Chebyshev (bottom-left), and Elliptic (bottom-right).

This research examines filters with the Butterworth, Chebyshev, and Inverse-Chebyshev responses. Each filter response contains various strengths and weaknesses (Maundy, 2005). The key strength of the Butterworth approximation is that its attenuation characteristic is almost truly maximally flat at the origin. However, its approximation to a flat response becomes progressively poorer as the angular frequency ($\omega$) becomes close to the passband edge angular frequency ($\omega_p$). The stopband attenuation of the Butterworth response is generally less than that obtainable from the Chebyshev response. For a given minimum stopband attenuation, an Inverse-Chebyshev filter will require a lower order than a Butterworth filter. The disadvantage of the Inverse-Chebyshev response concerns increased circuit realization complexity when designing band-elimination topologies.

To provide a diverse set of frequency responses and optimize the aggregate performance of these frequency filtering algorithms, each of the Butterworth, Chebyshev, and Inverse-Chebyshev responses are implemented. In MATLAB, filters of any order and type are created by determining the coefficients of the filter's transfer function. These coefficients are determined by MATLAB when input parameters such as the passband edge frequency, stopband edge frequency, and filter order are provided.

For an *n*-order filter of any type, MATLAB calculates the coefficients $a_1$, $a_2$, $a_{3...}a_{n+1}$, and $b_1$, $b_2$, $b_{3....}b_{n+1}$, used in

$$T(s) = \frac{B(s)}{A(s)} = \frac{b_1 s^n + b_2 s^{n-1} + b_3 s^{n-2} + \ldots b_{n+1}}{a_1 s^n + a_2 s^{n-1} + a_3 s^{n-2} + \ldots a_{n+1}}, \quad (1)$$

which represents a filter's transfer function. In equation 1, *s* is the Laplace operator and $s = i\omega$ for sinusoids ($\omega$ is the angular frequency in rad/s).

*Low-pass filter*

As one of the classifying techniques, a fourth-order Inverse-Chebyshev low-pass filter with a stopband edge angular frequency of 628 rad/s (corresponding to a frequency of 100 Hz) is implemented in MATLAB. Each channel in a microseismic event file is passed through this low-pass filter. The filtered output is analyzed for its peak amplitude. If this peak normalized amplitude is higher than an empirically determined value, the channel is assigned as passing this algorithm and having a "good" characteristic. Figure 5 depicts the frequency response of this filter. Figures 6 and 7 depict "good" and noise events, respectively, before and after this low-pass filter is applied. Notice the higher amplitude of the filtered "good" signal versus that of the noise signal.

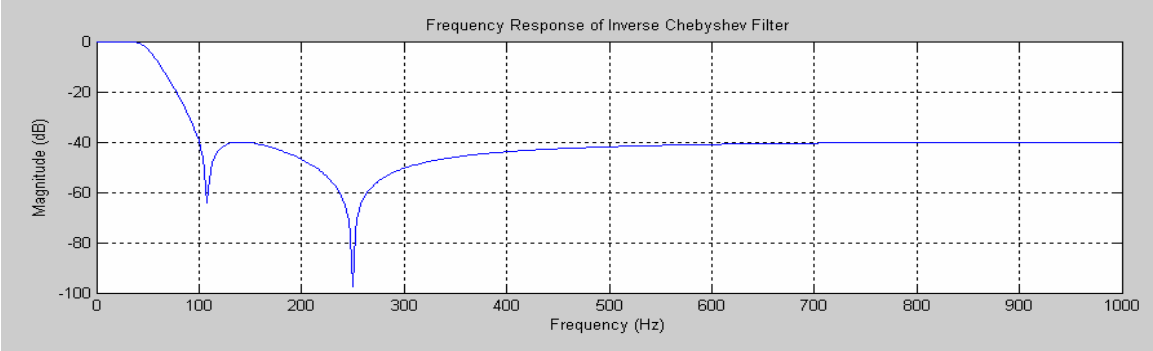


FIG. 5. Frequency response of the low pass Inverse Chebyshev filter used.

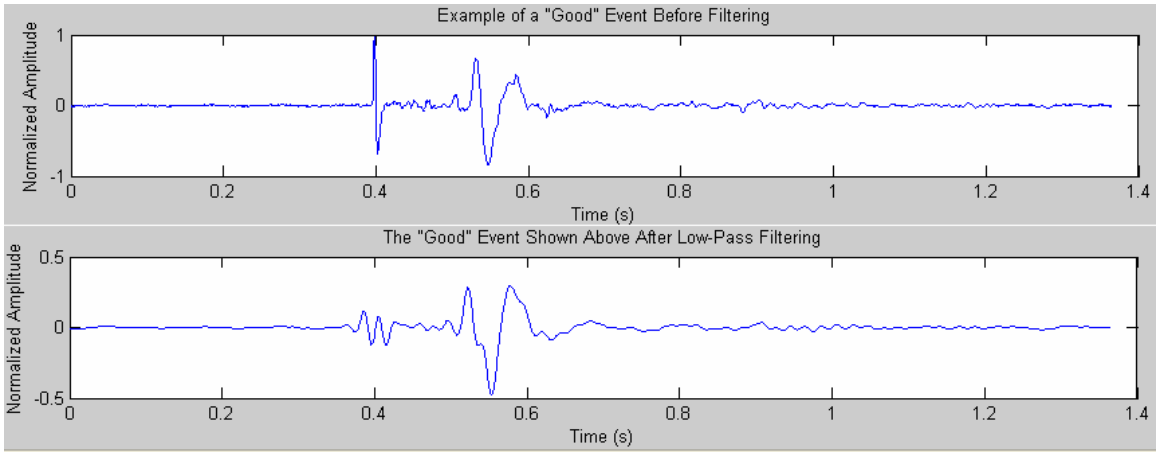


FIG. 6. A “good” event before (top), and after (bottom) low-pass filtering.

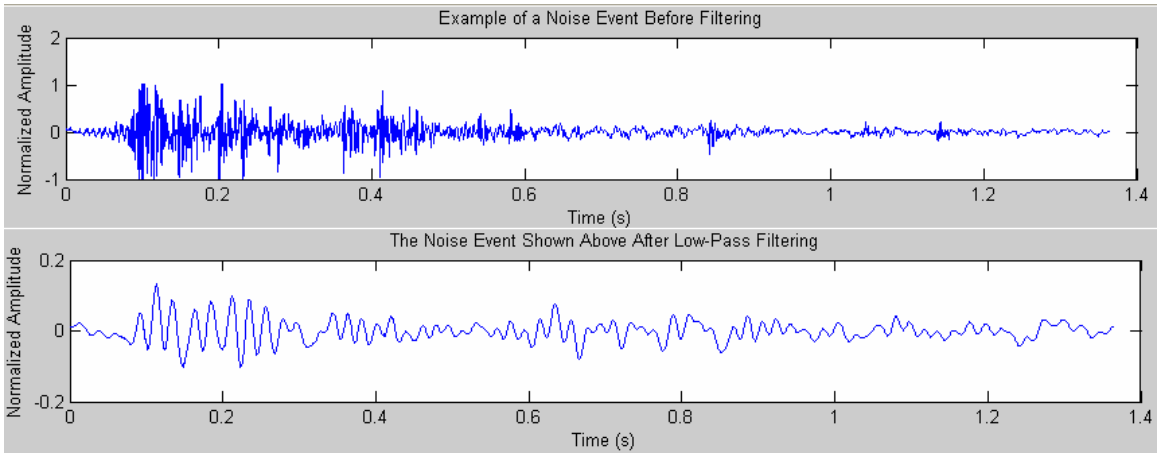


FIG. 7. A noise event before (top), and after (bottom) low-pass filtering.

*High-pass filter*

Another filter used in these classification algorithms is a fourth-order, high-pass filter with a Butterworth frequency response containing a passband with a lower limit of 2500 rad/s (398 Hz). Each channel in a microseismic event file is passed through this filter. The filtered output is analyzed for its peak amplitude. If this peak normalized amplitude is lower than an empirically determined setting, the channel is assigned as passing this algorithm and having a "good" characteristic. Figure 8 depicts the frequency response of this high pass filter. Figures 9 and 10 depict “good” and noise events, respectively, before and after this high-pass filter is applied. Notice the lower amplitude of the filtered “good” signal versus that of the noise signal**.**

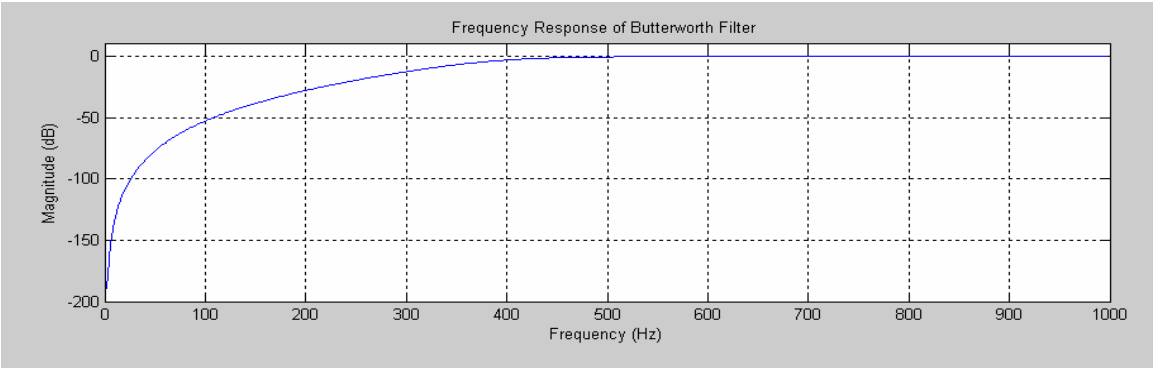


FIG. 8. Frequency response of the high pass Butterworth filter used.

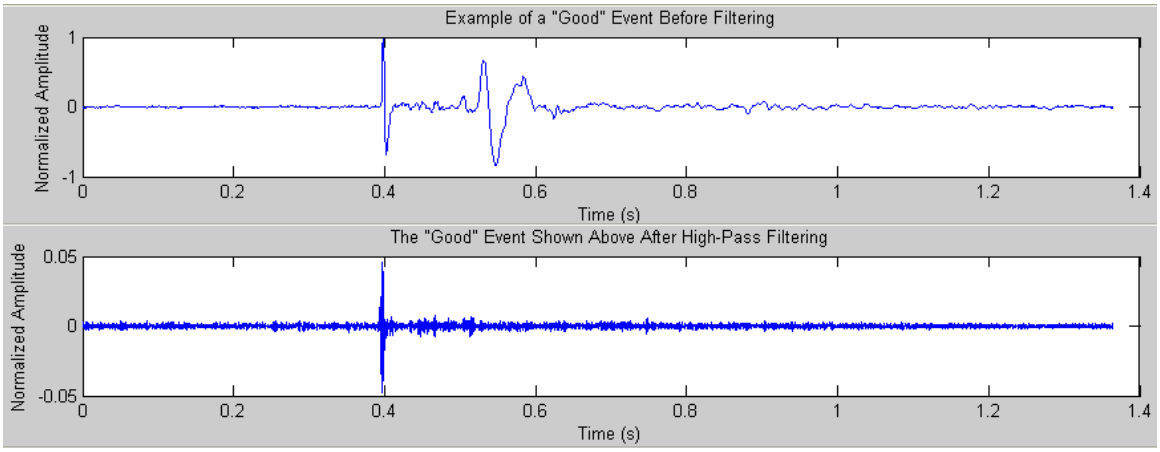


FIG. 9. A “good” event before (top), and after (bottom) high-pass filtering.

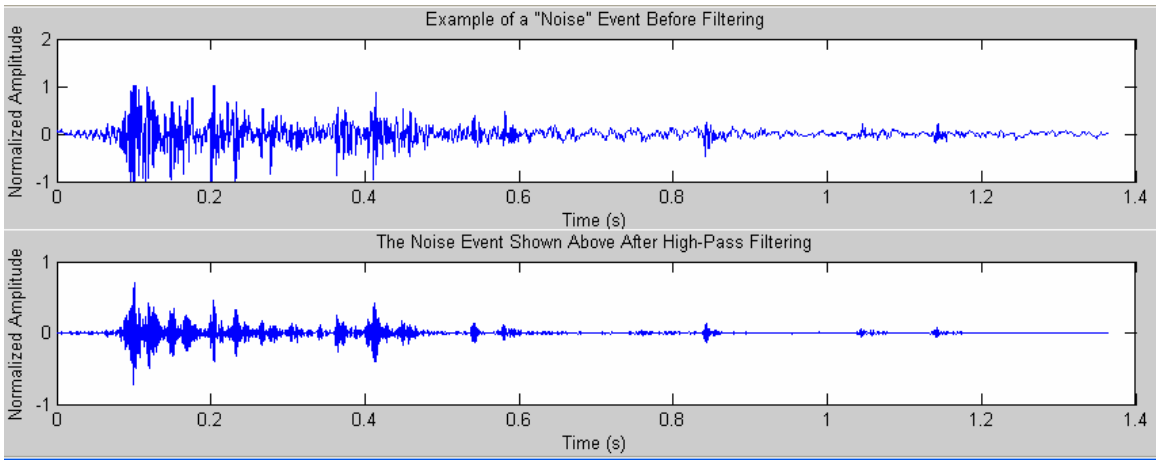


FIG. 10. A noise event before (top), and after (bottom) high-pass filtering.

*Band-pass filter*

The last filter used in the frequency filtering algorithms is a fourth-order, Chebyshev band-pass filter with a moderately high frequency passband ranging from 1000 rad/s to 2000 rad/s (159 Hz to 318 Hz). As each channel is examined, the filtered output is analyzed for its peak amplitude. If this peak normalized amplitude is lower than an empirically determined value, the channel is assigned as passing this algorithm and having a "good" characteristic. Figure 11 depicts the frequency response of this filter. Figures 12 and 13 depict “good” and noise events, respectively, before and after this band-pass filter is applied. Notice the lower amplitude of the filtered “good” signal versus that of the noise signal.

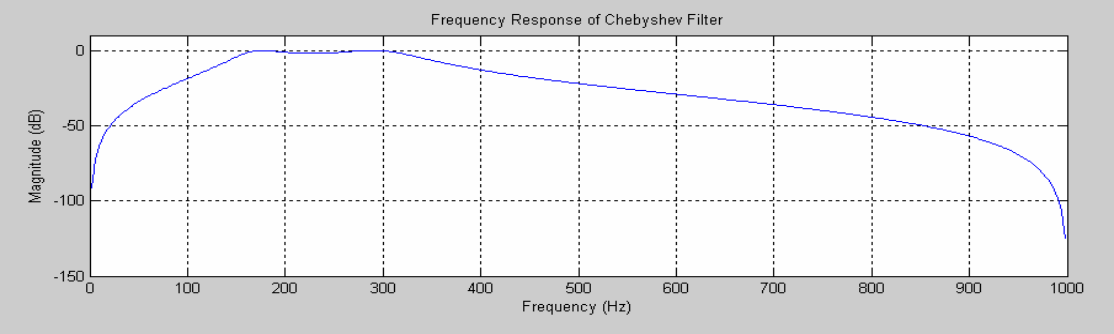


FIG. 11. Frequency response of the Chebyshev band pass filter used.

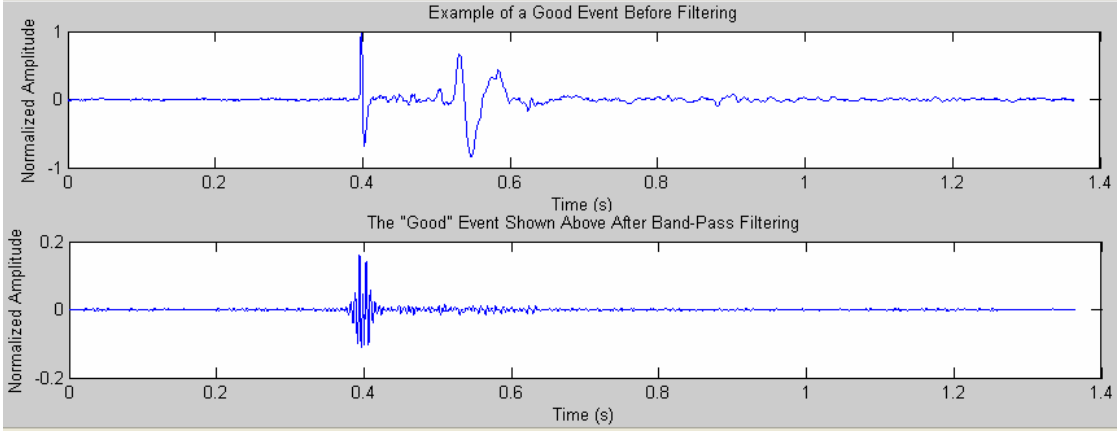


FIG. 12. A “good” event before (top), and after (bottom) band pass filtering.

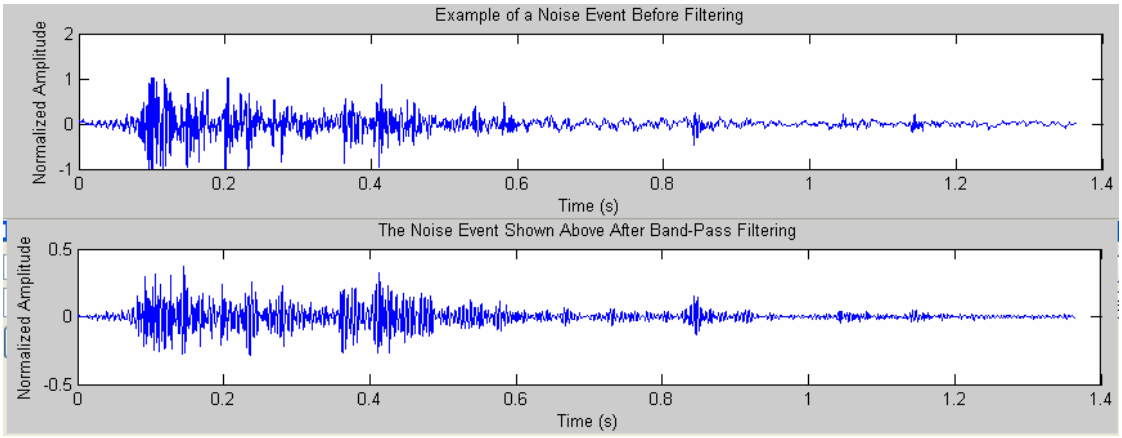


FIG. 13. A noise event before (top), and after (bottom) band pass filtering.

## Event length detection

Throughout this research, it is empirically determined that the event length of a detected microseismic earthquake is also a key determining characteristic of whether this event is worth further investigation (a "good" event) or not (a noise event). In general, the P-wave event length of a "good" event is significantly shorter than the event length of a noise event. Two algorithms are explored to determine the event lengths. The first algorithm is performed in the time-domain, and the second corresponds to a technique performed in a continuous-time frequency-domain.

### *Time-domain*

The time-domain algorithm explored is based on the STA/LTA algorithm (Ambuter and Solomon, 1974) demonstrated by Munro (2005). This algorithm looks at the energy contained in the signal at each point and performs short term averages and long term averages of these energies. This technique is known as the STA/LTA technique (short term averages divided by long term averages of the energy). In microseismic analysis, the STA/LTA ratio will significantly increase at the onset of a seismic event. Conversely, this ratio will significantly decrease at the termination of the seismic event. Thus, calculating the time differences between the onset and termination of the microseismic events yields the event length.

The STA can be defined as a quantity $\alpha(\tau)$, and the LTA can be defined as a quantity $\beta(\tau)$. A quantity $n_1$ corresponds to the number of samples taken in the STA window, and a quantity $n_2$ corresponds to the number of samples taken in the LTA window ($n_2 > n_1$). The value $E_e(t_k)$ corresponds to the signal energy at each time point $t_k$. The quantities $\alpha(\tau)$ and $\beta(\tau)$ can then be defined as

$$\alpha(\tau) = \frac{\sqrt{\sum_{-n} E_e(t_k)}}{n_1} \quad , \quad \beta(\tau) = \frac{\sqrt{\sum_{-n} E_e(t_k)}}{n_2} \; . \tag{2}$$

Using an algorithm similar to this STA/LTA technique, event lengths can be found. If the calculated event length of the channel being analyzed is less than an empirically

determined value, then the channel is assigned as passing this algorithm and having a "good" characteristic.

***Frequency-domain***

Through general observation, the high-frequency content of a microseismic signal significantly increases at the onset of the event and significantly decreases at the termination of the event. Thus, another method to pick the onset and termination of microseismic events is to continually analyze the frequency characteristics of a select number of points in the channel. If a time window is defined from $t_1$ to $t_2$ in the channel, a continuous-time frequency analysis can be performed by supplying a moving time window that exists between $t_1$ and $t_2$, with the limits $t_1$ and $t_2$ continuously increased up until the end of the channel data. Frequency characteristics are determined using the Fourier transform, defined as (Haykin, 2001):

$$G(f) = \int_{-\infty}^{\infty} g(t)\exp(-j2\pi ft)dt. \tag{3}$$

The function *g(t)* represents the sample points in the microseismic channel between the intervals $t_1$ and $t_2$, explained above. Thus, as $t_1$ and $t_2$ are continuously increased, a continuous time Fourier transform is performed. A normalized power spectral density, $|G(f)|^2$ is obtained using this algorithm and it is examined to determine the onset and termination times of the microseismic events.

Figure 14 depicts a "good" microseismic event in the time domain, and Figure 15 displays this event when the continuous time Fourier transform algorithm described above is applied to it. The onset and termination points of the P-wave arrival are shown in the figures. In Figure 15, the highest magnitudes are indicated with bright red and the lowest magnitudes are indicated with dark blue. Notice the sharp increase in high frequency content at the onset of the event, and the sharp decrease in high frequency content at the termination of the event. Figures 16 and 17 depict a rod noise microseismic event in the time, and continuous time-frequency domains, respectively.

When using this method, if the calculated event length of the channel is less than an empirically determined value, then the channel would be assigned as passing this algorithm and having a "good" characteristic.


FIG. 14. Time domain plot of an example microseismic “good” event.

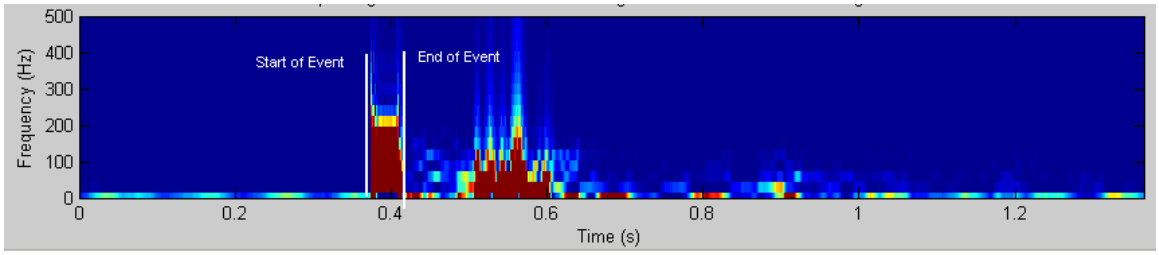


FIG. 15. Continuous time Fourier transform magnitude plot of Figure 14.

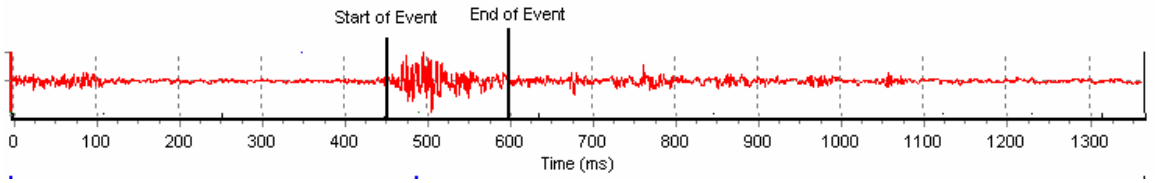


FIG. 16. Time domain plot of an example microseismic rod noise event**.**

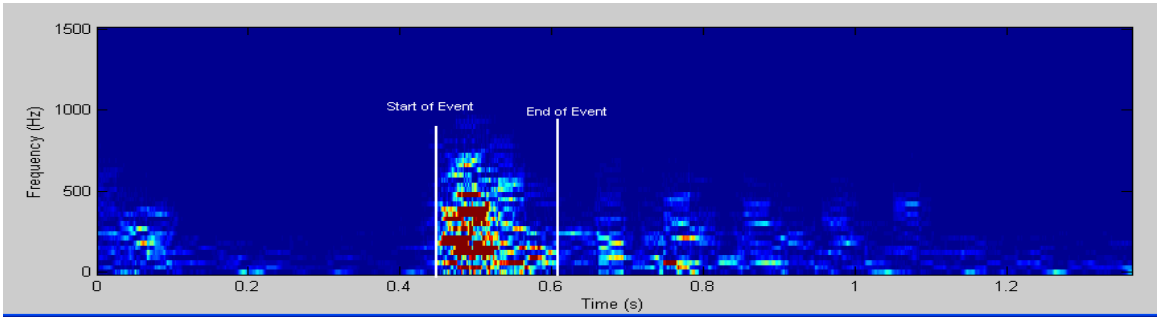


FIG. 17. Continuous time Fourier transform magnitude plot of Figure 16.

## Statistical analysis

Various statistical analysis techniques are explored. From observation, noise events generally oscillate more frequently about the time axis than "good" events. “Good” events are generally “flatter” and contain many data points that are close to the time axis.

One statistical algorithm examines the fraction of data points in the trace that are of reverse polarity compared to its preceding (or following) data point. In other words, as *n*, representing a single data point in the channel, is increased from 1 to the number of

sample points in the channel, this algorithm counts the total number of times that that the condition $[t_n t_{n+1} < 0]$ is satisfied. Let $N$ represent the total number of data points in the channel of interest. Essentially, this algorithm looks at the number of zero crossings in the channel and divides that value by the number of points in the channel. This quantity ($M$) is calculated using

$$M = \frac{\sum_{n=1}^{N-1}[(t_n t_{n+1}) < 0]}{N} \quad . \tag{4}$$

The quantity $[t_n t_{n+1} < 0]$ is equal to 1 if this condition is satisfied and 0 if it is not.

If $M$ is less than an empirically determined value, then the channel is assigned as having a "good" characteristic. As an example of an application of this algorithm, the "good" event shown in Figure 2 has $M$ = 0.00024414, and the noise event shown in Figure 3, has $M$ = 0.0728.

Another statistical algorithm separates all of the data points of the trace into 99 separate bins that are evenly spaced between normalized data values of -1 and 1. It then examines the 50$^{th}$ bin and looks at the percentage of data points that are contained in that bin. If that percentage is greater than an empirically determined percentage, then the channel is assigned as passing this algorithm and having a "good" characteristic. Figure 18 shows this histogram for the "good" channel shown in Figure 2, while Figure 19 shows this histogram for the noise channel shown in Figure 3. Notice the much higher concentration of points in the middle bin for the "good" channel.

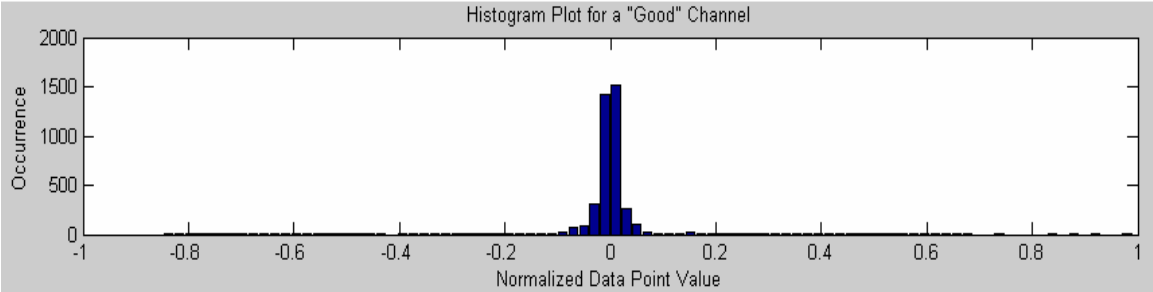


FIG. 18. Histogram plot of an example “good” channel.

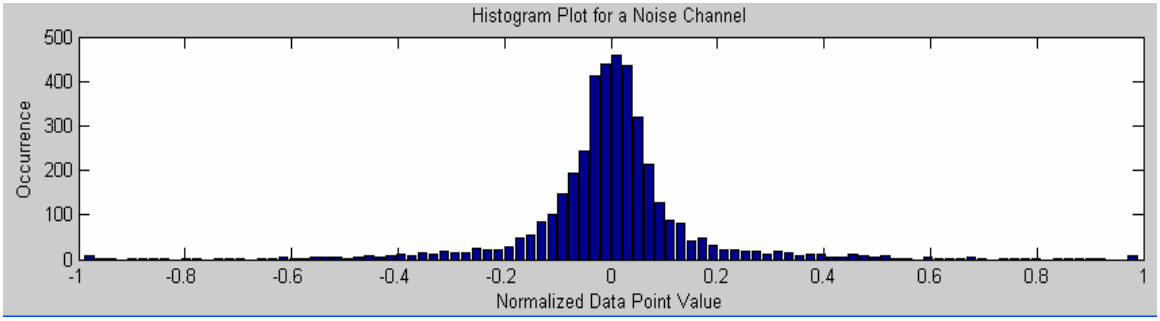


FIG. 19. Histogram plot of an example noise channel.

## Other algorithms

Other classification algorithms were researched throughout this project including coherence, semblance, and cross-correlation techniques, as depicted in Sheriff and Geldart (1995). However, after testing these algorithms on microseismic data, it was found that the classification accuracy of these techniques was not as high as desired. Thus, these techniques are not implemented in the MATLAB program.

# IMPLEMENTATION

Many of the discussed algorithms are combined and optimized. An interactive and fully automated MATLAB Graphical User Interface (GUI) application is created that allows the user complete control of the discriminating thresholds in the algorithms. In addition, statistical plots and histograms are dynamically available so that the user can adjust the settings of the program to accommodate a wide variety of data sets and track the algorithmic characteristics of every channel in every file examined. This application, entitled "Event_Analyzer", classifies and separates microseismic event files into noise events and “good” events. It is also capable of plotting spectrograms (frequency content plots that vary with time) for further analysis. Figure 20 depicts the appearance of this GUI upon program start-up.

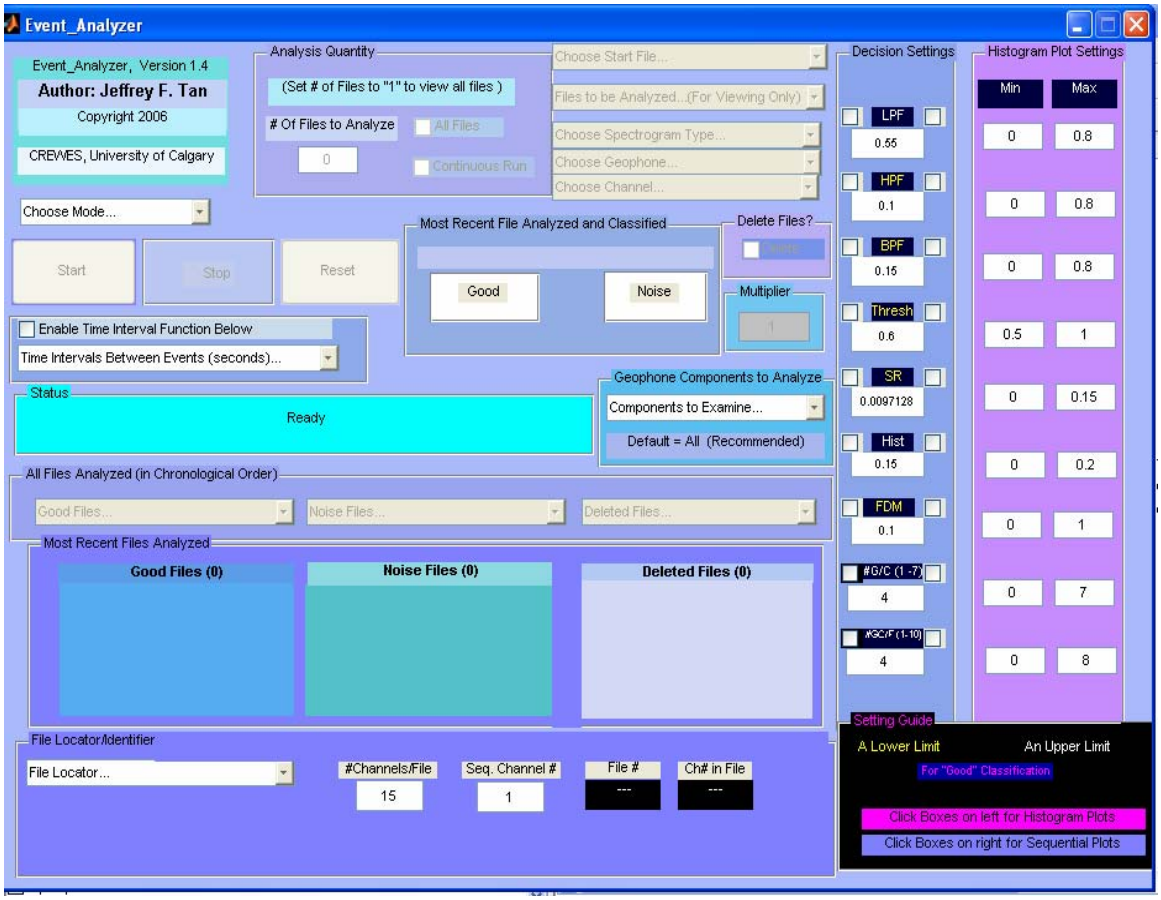


FIG. 20. Event_Analyzer program upon start-up.

## RESULTS

This program is currently undergoing testing. Preliminary tests have yielded reasonably strong results. The end goal of this research is to have this program eventually implemented on the Imperial Oil passive seismic monitoring system at Cold Lake, Alberta. The magnitude of the economic impact of this GUI application, should it be implemented, would be the result of a much higher microseismic file classification accuracy for the thousands of microseismic files (at least) that are generated every day at the large heavy oil production area of Cold Lake, Alberta. Thus, microseismic files from potentially undesirable seismic events caused by various production issues would be much easier to find and prompt action would be possible; furthermore, a potential shift in focus from manual microseismic file examining to other pertinent production issues could occur.

## CONCLUSIONS

Microseismic classification algorithms that include frequency filtering, event length detection, and statistical analysis are explored and a MATLAB Graphical User Interface (GUI) application is created and tested on files generated from the passive seismic monitoring system at Cold Lake, Alberta. Preliminary tests have yielded reasonably strong results. Much testing remains to be done, however. The end goal of this research is to have this program (entitled "Event_Analyzer") implemented on this Cold Lake passive seismic monitoring system.

## ACKNOWLEDGEMENTS

We would like to thank the entire CREWES staff for providing us with help whenever needed. We are also thankful to Colum Keith, Richard Smith, and Sophia Follick of Imperial Oil Ltd. who provide data and innovative tasks, are performing a wide variety of testing on the program, and are consistently providing valuable feedback.

## REFERENCES

Ambuter, B.P. and Solomon, S.C., 1974, An event-recording system for monitoring small earthquakes: Bulletin of the Seismological Society of America, **64**, 1181-1188.

Campbell, G., 2005. Velocity Model Improvements for use in Imperial Oil's Microseismic Analysis Program: Imperial Oil Resources & University of Alberta.

Geldart, L.P. and Sheriff, R.E., 1995, Exploration Seismology, 2nd edition: Cambridge University Press.

Haykin, S., 2001, Communication Systems, 4th edition: John Wiley & Sons.

Imperial Oil Ltd, 2006, Proposed Development Areas – Mahihkan North and Nabiye: http://www.limperiale.ca/Canada-English/Investors/Operating/Natural_Resources/I_O_NaturalResourcesFig4.asp, internet web page.

Maundy, B., 2005, ENEL 559 Course Notes, University of Calgary.

Munro, K. A., 2005, Analysis of microseismic event picking with applications to landslide and oil-field monitoring settings: MSc. thesis, University of Calgary.